CONCENTRIC CRATER FILL IN THE CASIUS REGION OF MARS. Bryce A. Troncone,[1] Navaeh Sauceda,[2] Matthew R. Perry,[3] Aaron T. Russell,[3] Megan B. Russell,[3] and Nathaniel E. Putzig.[3] [1] Rutgers University (bat94@scarletmail.rutgers.edu), [2] Bear Creek High School, [3] Planetary Science Institute.

Introduction: Identifying and characterizing ice-rich landforms on Mars is an important scientific endeavor of the Mars science community [1]. Ample remote-sensing data exist confirming that Martian landforms such as lobate-debris aprons and lineated valley fills are forms of debris-covered glaciers (DCG) [2, 3]. One particular type of DCG, concentric crater fill (CCF), is observed within many high- and mid-latitude craters and is thought to be composed of ice, dust, and rocky debris formed through glacial ice flow and recession [4,5]. Accumulations of CCF are estimated to reach hundreds to thousands of meters in thickness [6].

Glacial landforms including CCF were previously characterized and mapped between ~±30° and 50° latitude in both hemispheres [6]. However, questions remain regarding the volume fraction and distribution of water ice within CCF.

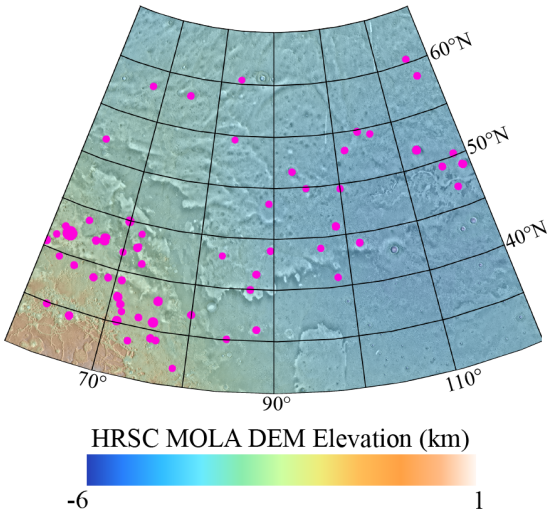

Figure 1: Study area showing CCF with surface areas ≥100 km² (magenta circles). Basemap is THEMIS 100 m/pixel daytime IR (grayscale) with HRSC-MOLA DEM Elevations as a color overlay.

In this project, we characterized CCF with total surface areas ≥100 km² [6] (Fig. 1) within the MC-06 "Casius" quadrangle using various remote sensing datasets. We aim to improve understanding of the appearance, composition, and state of degradation of these larger CCF and begin building a global catalog of CCF characteristics.

Methods: We take a holistic approach to analyzing remote-sensing data with various sensing depths to provide a clearer understanding of the landforms under investigation. In this study, we used optical imagery from the Context Camera (CTX) [7] and High-Resolution Imaging Science Experiment (HiRISE) [8] for surface geomorphic characterization. We then used thermal inertia (TI) modeling [9] reliant on temperature measurements from the Thermal Emission Spectrometer (TES) [10] and the Thermal Emission Imaging System (THEMIS) [11] to constrain properties of the upper decimeter of the CCF material. Layers of high TI material are consistent with ice or ice-cemented ground. To extend assessment of properties through the upper ~5 m of the subsurface, we used Mars Shallow Radar (SHARAD) surface power returns (SSPR) [12], where low power is an indicator of low density that may be consistent with ice. Finally, we identified subsurface reflections in SHARAD observations to assess the deeper interior of each CCF [13]. Such reflections are often associated with the base of glacial and ground ices.

Preliminary Results: We investigated 61 craters in the Casius region with diameters of 10-64 km. The highest abundance of CCF within our study area occurs along the global dichotomy boundary, in the southwest corner of the region. Flow channels are prevalent in CCF near or along the Martian dichotomy, with the most significant ones occurring west of ~90° E and south of ~45° N.

Geomorphology: Out of 61 craters studied, 17 contain significant flow channels, and 55 contain brain terrain, polygonal ice patterns, and/or concentric ridge features consistent with an ice-rich subsurface. This morphology has been previously reported to occur within CCF [4].

Thermal Inertia: Using MARSTHERM, an online set of thermophysical analysis tools [14], we modeled seasonal apparent TI for a pair of craters with low SSPR and compared to TES data. Solar longitudes of 120-160° are specified to avoid seasonal CO_2 frost [9]. The results over both craters are indicative of a thin, high-TI material overlaying a low-TI material. TES-derived TI for crater one (~288° W, ~35° N) averages ~150 tiu, modeled with a 1.9 cm thick high-TI duricrust over low-TI dust, while that of crater two (~243° W, ~58.5° N) averages ~250 tiu, modeled with a 0.9 cm high-TI duricrust over lower-TI sand. These results are consistent with seasonal TES data stamps that display variations of several hundred tiu within the craters. At least in these cases, the thermal data does not appear to be probing deeply enough to sense an ice table.

SHARAD Surface Power Returns: We extracted the SSPR from CCF and non-ice related materials and compared their histograms. The CCF material exhibits a ~2 dB lower SSPR than the non-ice related material in the Casius region (Figure 2).

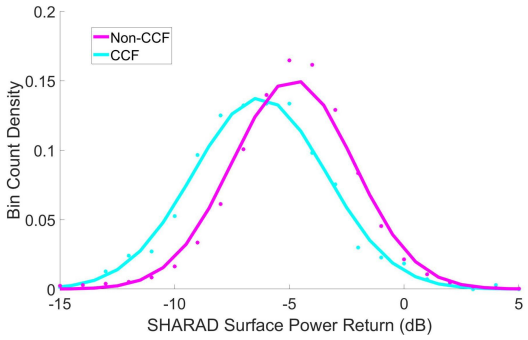

Figure 2: Probability Density Function of CCF and non-CCF material surface power returns in the Casius region. Histogram bin centers are displayed as asterisks.

SHARAD Subsurface Returns: Despite the difficulties that radar analysis within craters usually poses, ~40 out of the 61 CCF analyzed contained high-confidence subsurface reflections ranging in depth from ~15 m to ~1300 m (assuming a real permittivity of 3.15, that of pure ice). Our confidence in mapping reflectors is based on clutter discrimination and whether the estimated depth to the reflector is within the bounds of the expected crater morphology.

Discussion: Low SSPR within CCF, when compared to non-CCF material, indicates the presence of low-density material such as ice or a mixture of ice and sediment infill within the upper 5 m [12]. Conversely, a different material such as dust may account for the low density. Our geomorphic analysis shows that CCF have varying levels of degradation, suggesting the amount of water ice within CCF may be controlled by local conditions. The interpretations of our geomorphic and SSPR work are broadly consistent with previous studies suggesting an ice-rich composition of CCF material, e.g., [4].

Many prior studies have either omitted a radar component or have not identified any significant subsurface reflections within CCF [6,15,16,17]. We found that ~⅔ of the CCF investigated contain at least one subsurface reflector, although some of our detections may be due to surface clutter that is not resolved in MOLA-based cluttergrams [18]. Future studies should consider investigating subsurface signatures of ice using radar, and if possible, use a higher resolution DEM to produce cluttergrams.

Pure ice has a TI of 2000-2500 tiu [19], similar to that of bedrock. The limited thermal modeling in this study finds layers with lower TI values and a stratigraphy that is inverted relative to that expected for buried ice (i.e., low TI over high TI). Our results place a modest constraint on overburden characteristics at two sites, providing a starting point for work that could be extended to other study sites.

Conclusion: We analyzed the CCF within the Casius (MC-06) region that have surface areas ≥100 km^2 using various remote datasets. Our study confirms the ice-rich nature of these landforms. However, more detailed analyses and modeling of these features are needed to place better constraints on their water-ice volume as well as the potential overburden thickness. Additional work may include the utilization of a multilayered TI derivation to improve constraints on the stratigraphy and thermal properties of the upper meters of CCF. Higher-resolution SHARAD cluttergrams would enable more thorough clutter discrimination and bolster the interpretation of potential subsurface reflectors. Enhanced geomorphic analyses of the CCF would aid further investigation into the distribution of landforms within CCF material. Extending the use of all datasets in this study to the entire Casius quadrangle would provide a better assessment of the geospatial dependence on CCF, thereby informing formation and erosional mechanisms that control CCF characteristics.

Acknowledgments: This work was supported by the NASA Summer Undergraduate Program for Planetary Research (SUPPR) and the LPI Cooperative Agreement, and the Jefferson County Colorado Executive High School Internship Program. SHARAD subsurface reflection data were processed using CO-SHARPS [20]. We are grateful to Gareth Morgan for providing the SHARAD surface-power data.

References: [1] Banfield D. ed. (2020) *MEPAG*. [2] Head J. W. et al. (2006) *Earth & Planet. Sci. Lett*, 241:663-671. [3] Holt J. W. et al. (2008) *Science*, 322:1235-1238. [4] Levy J. S. et. al. (2010) *Icarus*, 209:390–404. [5] Fastook, J. L. and Head, J. W. (2014) *Planet. & Space Sci*, 91:60-76. [6] Levy J. S. et al. (2014) *JGR:Planets*, 119:2188-2196. [7] Malin M. C. et al. (2007) *JGR*, 112:E05S04. [8] McEwen A. S. et al. (2007) *JGR*, 112:E05S02. [9] Putzig N. E. and Mellon M. T. (2007) *Icarus*, 191:68-94. [10] Christensen P. R. et al. (2001) *JGR:Planets*, 106:23823-23871. [11] Christensen P. R. et a. (2004) *Space Sci. Rev.*, 110:85-130. [12] Morgan G. et al (2021) *Nat. Astron.* 5:230-236. [13] Seu R. et al. (2007) *JGR*, 112:E05S05. [14] Putzig, N. E. et al. (2013) *AGU XLVI*, Abstract #P43C-2023. [15] Sejourne A. et al. (2018) *JGR:Planets*, 124:483-503. [16] Gallagher C. et al. (2021) *Icarus*, 355:114173. [17] Jawin E. R. and Head J. W. (2021) *Icarus*, 355:114117. [18] Cook C. W. et al. (2020) *Icarus*, 348:113847. [19] Mellon M. T. et al. (2008) *The Martian Surface*, ch.18:399-427. [20] Putzig N. E. et al. (2016) LPSC XLVII, Abs. 3010.